Analysis of MMC Dynamics in dqz Coordinates for Vertical and Horizontal Energy Balancing Control

Gilbert Bergna-Diaz *, Julian Freytes §, Xavier Guillaud ‡, Salvatore D'Arco † and Jon Are Suul †
* Norwegian University of Science and Technology - Trondheim, Norway
§ Grid Solutions, GE Power - Massy, France
‡ Université Lille, Centrale Lille, Arts et Métiers, HEI - EA 2697 - L2EP - Lille, France
† SINTEF Energy Research - Trondheim, Norway

***Abstract*—This paper presents a control system implementation in dqz-coordinates for equalizing the average energies stored in each arm of a Modular Multilevel Converter (MMC); a control objective that is typically referred to as horizontal and vertical energy balancing. The proposed control scheme is obtained from analysis and simplification of a detailed time-invariant dqz-frame state-space representation of the MMC. The state variables of the model are the equivalent arm capacitor energies and the current components, and it will be shown that this representation is very suitable for designing outer-loop energy controllers in dqz coordinates that rely on linear inner current control loops. Moreover, a series of justified assumptions on the energy dynamics will be presented, providing significant insight that simplifies the control design. Finally, by proving that the unbalances of the average values of the converter equivalent arm capacitor energies in abc coordinates appear as undesired oscillations in dqz coordinates, active filtering is proposed as a mean to dissipate them and, therefore, achieve the desired balanced operation. Operation of the proposed control strategy is demonstrated by time-domain simulation of a 1 GW MMC-based HVDC converter terminal.**

***Index Terms*—Energy Balancing Control, Modular Multilevel Converters, HVDC Transmission.**

I. Introduction

The Modular Multilevel Converter (MMC) is normally operated to ensure that the total energy stored in each of the arms will be approximately balanced in average. The energy balance between the arms and phases of the MMC, combined with the balancing of the sub-module (SM) voltages within each arm, is necessary for limiting the voltage stress on the switching devices and SM capacitors of the converter [1], [2]. For ensuring equal average energy in all arms, the MMC control system should ensure balancing of the energy between the phases, referred as horizontal balancing, and the balancing of the energy between the upper and lower arms in each phase, referred as vertical balancing [3].

The energy balancing of MMCs is especially critical when compensation of the arm capacitor voltage variations is included in the calculation of the insertion indices [2], [4]. This approach has been labelled as "Compensated Modulation" (CM) in [5], [6], and implies a partial feedback linearization with respect to the current dynamics of the MMC. Under CM, linear inner current control loops perform notably well [5], [7], but the MMC loses its self-stabilizing properties, and dedicated control loops for balancing the average arm voltages or energies are necessary to preserve stable operation [2], [4], [5]. As an opposite approach, the control can be based on linear current loops without compensation for variations in the equivalent arm capacitor voltages, referred to as "Un-Compensated Modulation" (UCM) in [8]. Albeit the performance of such control systems are more affected by non-linearities, it is well known that they are naturally self-stabilizing [9], [10] and can operate without any outer energy control loops. However, it has been proven in [11] that explicit energy control can improve the stability margins, dynamic performance, and robustness.

Several methods for energy-based control and balancing of the average values of the MMC arm energies have been proposed in the literature [2]–[4], [7], [12]–[18]. However, with the notable exceptions of [12], [17], these control strategies have been designed in the stationary frame and implemented with abc coordinates, possibly due to the lack of suitable models in dqz coordinates. The control strategy in [12] was designed in a set of dqz reference frames, but depended on multiple decoupling networks for extracting the different frequency components appearing in the MMC variables. Instead, [17] translated and adapted an energy balancing control strategy originally designed in the stationary abc reference into dqz coordinates. Thus, both these proposals resulted in relatively complex control schemes.

Detailed steady-state time-invariant (SSTI) state-space representation of MMC dynamics in dqz coordinates have been only recently derived, as documented in [6], [19] and references therein. Such SSTI models are suitable for traditional eigenvalue-based analysis of stability and parameter sensitivity [20], and can be applied for design of advanced controllers that require the knowledge of a constant equilibrium in steady-state operation, such as LQR methods [21], [22]. However, application of simplifications or model reduction techniques to detailed SSTI models can also reveal system properties that are useful for conventional control system design.

Starting from the SSTI MMC model for CM presented in

The work performed by SINTEF was partly supported by the EU FP7 project BestPaths - Beyond State-of-the Art Technologies for Repowering AC Corridors and Multi-Terminal HVDC Systems, under Grant Agreement No 612748, and partly by the project HVDC Inertia Provision (HVDC Pro), financed by the ENERGIX program of the Research Council of Norway (project number 268053/E20) and the industry partners; Statnett, Equinor, RTE and ELIA.

This is the accepted version of a paper published in 44th Annual Conference of the IEEE Industrial Electronics Society (IECON2018)
DOI: 10.1109/IECON.2018.8592881

[6], this paper introduces a set of justified assumptions and simplifications that provide further insights on the mutual dynamic couplings between frequency components. Furthermore, it is demonstrated that unbalanced dc components in the arm capacitor energies appear as undesired oscillations in the dqz coordinates. Then, the paper develops two control schemes based on dq-frame active damping of these oscillations to remove energy unbalances. Finally, these control schemes are validated with numerical simulation based on an established average arm model (AAM) of an MMC in the stationary abc frame [4], [23].

II. Mathematical Modelling of MMCs

This section defines the modelling conventions adopted in the paper and recalls the mathematical state-space $\Sigma\Delta$ representation of the MMC in abc and dqz coordinates.

A. Modeling conventions

The basic topology of a three-phase MMC is displayed in Fig. 1 where the series connection of N SMs with capacitors C constitute one arm of the converter. The arms are connected to a filter inductor with inductance L_σ and equivalent resistance R_σ to form the connection between one of the dc-terminals and the ac-side output. Two identical arms are connected to the upper and lower dc-terminals, respectively, to form one leg for each phase $j \in \{a, b, c\}$. The ac-side interface is assumed to be a filter inductor and/or the leakage inductance of a transformer, which is modeled by an equivalent inductance L_f and resistance R_f.

Assuming that the capacitor voltages of the SMs are maintained well balanced within the arms, the series connection of SMs in each arm can be replaced by a circuit-based average model with $v_{C_j}^{U,L} = \sum_{i=1}^{N} v_{\mathrm{SM}j,i}^{U,L}$ and $C_\sigma = C/N$, corresponding to the well-known AAM [4], [24]. Thus, each arm can be represented by a power-balance-based average model of a single-phase VSC, with a modulated voltage source interfacing the filter inductor, and a controlled current source interfacing the capacitor-side, as shown for the lower arm of phase c in Fig. 1.

The output of the controlled voltage sources of the AAM are here referred to as the modulated voltages v_{Mj}^U and v_{Mj}^L, which are respectively related to the equivalent arm capacitor voltages v_{Cj}^U and v_{Cj}^L by means of the equivalent insertion indices m_j^U and m_j^L through the relationships $v_{Mj}^U = m_j^U v_{Cj}^U$ and $v_{Mj}^L = m_j^L v_{Cj}^L$. Moreover, the energy of the equivalent arm capacitors are directly computed as $w_{Cj}^{U,L} = \frac{1}{2} C_\sigma (v_{Cj}^{U,L})^2$. Finally, the upper and lower arm currents associated with L_σ are denoted by i_j^U and i_j^L, the ac-grid current associated to L_f is denoted as i_j^Δ, and v_{Gj}^Δ is the grid voltage at the ac-side point of common coupling.

B. MMC Σ-Δ representation in abc coordinates

As demonstrated in [2], [4], [6], [19], it can be convenient to adopt a Σ-Δ representation instead of an Upper-Lower (U-L) arm notation. Thus, the following definitions are introduced:

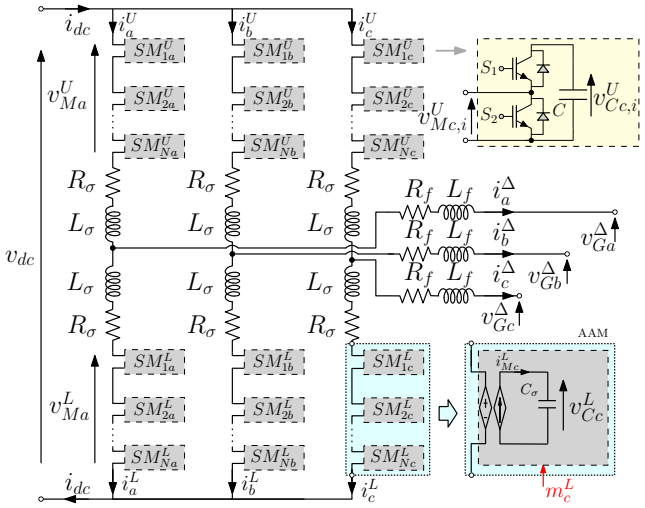

Fig. 1. MMC Topology and AAM (phase c).

$$
\begin{aligned}
i_{abc}^\Delta &\triangleq i_{abc}^U - i_{abc}^L, & i_{abc}^\Sigma &\triangleq \frac{i_{abc}^U + i_{abc}^L}{2} \\
w_{Cabc}^\Delta &\triangleq w_{Cabc}^U - w_{abc}^L, & w_{Cabc}^\Sigma &\triangleq w_{Cabc}^U + w_{Cabc}^L \\
v_{Mabc}^\Delta &\triangleq \frac{v_{Mabc}^L - v_{Mabc}^U}{2}, & v_{Mabc}^\Sigma &\triangleq \frac{v_{Mabc}^L + v_{Mabc}^U}{2}
\end{aligned} \tag{1}
$$

In (1), i_j^Σ is the circulating or common-mode current, w_{Cj}^Δ and w_{Cj}^Σ are the difference and sum of the equivalent upper and lower arm capacitor energies, respectively, while v_{Mabc}^Δ and v_{Mabc}^Σ are the difference and sum between the upper and lower modulated voltages [6].

With the definitions in (1), and by applying Kirchhoff's voltage and current laws to the circuit in Fig. 1, it is possible to represent the converter dynamics as:

$$
\begin{aligned}
\dot{w}_{Cabc}^\Sigma &= -v_{Mabc}^\Delta \circ i_{abc}^\Delta + 2 v_{Mabc}^\Sigma \circ i_{abc}^\Sigma \\
\dot{w}_{Cabc}^\Delta &= -2 v_{Mabc}^\Delta \circ i_{abc}^\Sigma + v_{Mabc}^\Sigma \circ i_{abc}^\Delta \\
L_\sigma \dot{i}_{abc}^\Sigma &= -R_\sigma i_{abc}^\Sigma + \mathbb{1}_3 \frac{v_{dc}}{2} - v_{Mabc}^\Sigma \\
L_\delta \dot{i}_{abc}^\Delta &= -R_\delta i_{abc}^\Delta + v_{Mabc}^\Delta - v_{Gabc}^\Delta
\end{aligned} \tag{2}
$$

where $\circ$ denotes the element-wise multiplication of vectors (e.g.: $[a] \circ [c] = [ac]$), $\mathbb{1}_3 \in \mathbb{R}^3$ is a vector of ones, and R_δ, L_δ are defined by $R_\delta \triangleq R_f + R_\sigma/2$ and $L_\delta \triangleq L_f + L_\sigma/2$.

C. MMC Σ-Δ representation in dqz coordinates

The state-space SSTI model of the MMC proposed in [6] is valid under the assumptions of CM. For the sake of completeness, the assumption of CM is recalled in A1.

A1. The arm insertion indices of the MMC are computed by compensating for the capacitor voltage oscillations of their corresponding arm:

$$
m_j^U = \frac{v_{Mj}^{U*}}{v_{Cj}^U}, \qquad m_j^L = \frac{v_{Mj}^{L*}}{v_{Cj}^L},
$$

with v_{Mj}^{U*} and v_{Mj}^{L*} being the arm voltage references.

This is the accepted version of a paper published in 44th Annual Conference of the IEEE Industrial Electronics Society (IECON2018)
DOI: 10.1109/IECON.2018.8592881

Remark 1: Under the assumption of CM, $v^{U*}_{Mabc} \equiv v^{U}_{Mabc}$ and $v^{L*}_{Mabc} \equiv v^{L}_{Mabc}$ which also imply that $v^{\Delta*}_{Mabc} \equiv v^{\Delta}_{Mabc}$ and $v^{\Sigma*}_{Mabc} \equiv v^{\Sigma}_{Mabc}$. Thus, under CM the modulated voltages in Σ-Δ coordinates, v^{Σ}_{Mabc} and v^{Δ}_{Mabc}, are suitable to consider directly as control variables instead of the insertion indices.

Remark 2: The equations expressing the current dynamics of the MMC are linear with respect to v^{Σ}_{Mabc} and v^{Δ}_{Mabc} while the equations expressing its capacitor energy dynamics remain non-linear as in (2). Moreover, these two variables do not appear in the capacitor voltage dynamics. Thus, under CM, it is more suitable to consider the capacitor energies as a state variables instead of the capacitor voltages.

Under the approximation A1, the MMC dynamics in SSTI dqz representation can be derived according to [6], as recalled here for convenience.

$$\begin{aligned}
\dot{w}^{\Sigma}_{Cdq} &= \mathcal{P}^{\Sigma}_{dq} + \mathbb{J}_2 2\omega w^{\Sigma}_{Cdq} \\
\dot{w}^{\Sigma}_{Cz} &= \mathcal{P}^{\Sigma}_{z}; \\
\dot{w}^{\Delta}_{Cdq} &= \mathcal{P}^{\Delta}_{dq} - \mathbb{J}_2 \omega w^{\Delta}_{Cdq}, \\
\dot{w}^{\Delta}_{CzDQ} &= \mathcal{P}^{\Delta}_{zDQ} - \mathbb{J}_2 3\omega w^{\Delta}_{CzDQ}
\end{aligned} \tag{3a}$$

$$\begin{aligned}
\dot{i}^{\Sigma}_{dq} &= -\frac{R_\sigma}{L_\sigma} i^{\Sigma}_{dq} - \frac{v^{\Sigma}_{Mdq}}{L_\sigma} + \mathbb{J}_2 2\omega i^{\Sigma}_{dq} \\
\dot{i}^{\Sigma}_{z} &= -\frac{R_\sigma}{L_\sigma} i^{\Sigma}_{z} + \frac{v_{dc}}{L_\sigma} - \frac{v^{\Sigma}_{Mz}}{L_\sigma} \\
\dot{i}^{\Delta}_{dq} &= -\frac{R_\delta}{L_\delta} i^{\Delta}_{dq} + \frac{v^{\Delta}_{Mdq}}{L_\delta} - \frac{v^{\Delta}_{Gdq}}{L_\delta} - \mathbb{J}_2 \omega i^{\Delta}_{dq}
\end{aligned} \tag{3b}$$

More precisely, the dynamics of the nonlinear capacitor energy dynamics are expressed by (3a), with $\mathcal{P}^{\Sigma}_{dqz}$, $\mathcal{P}^{\Delta}_{dq}$ and $\mathcal{P}^{\Delta}_{zDQ}$ representing nonlinear functions with power units. These terms consist of sums of products between the control voltages and MMC currents, and are respectively defined in (4a), (4b) and (4c), at the top of the next page. Furthermore, $\mathbb{J}_2 \in \mathbb{R}^2$ is defined as

$$\mathbb{J}_2 \triangleq \begin{bmatrix} 0 & 1 \\ -1 & 0 \end{bmatrix}.$$

The linear current dynamics are given directly by (3b).

Remark 3: It is worth highlighting that compared to the model originally presented in [6], the definitions of the modulated powers in (4) have been extended to include the possibility of a third harmonic injection by means of the definition $v^{\Delta}_{Mz} \triangleq v^{\Delta}_{MzD}\cos(3\omega t) + v^{\Delta}_{MzQ}\sin(3\omega t)$, following a similar procedure to the one proposed in [19].

III. Impact of steady-state dc unbalances on MMC energy components

The control schemes proposed in this paper are designed to eliminate steady-state dc unbalances between the energy variables in each arm. Such dc unbalances may occur in case of CM, or even under UCM suffering from parametric uncertainty. However, since the control is being designed in the dqz coordinates, it is first necessary to clarify how a dc unbalance between phases appears in dqz coordinates.

A. Steady-state energy variables in abc coordinates

The steady-state energy variables can be expressed as:

$$\begin{aligned}
w^{\Sigma\mathrm{ss}}_{Cabc} \triangleq & \overline{W}^{\Sigma\mathrm{ss}}_{C} \begin{bmatrix} \sin\left(2\omega t + \overline{\phi}^{\Sigma}_{\mathrm{ss}}\right) \\ \sin\left(2\omega t + \overline{\phi}^{\Sigma}_{\mathrm{ss}} + \frac{2\pi}{3}\right) \\ \sin\left(2\omega t + \overline{\phi}^{\Sigma}_{\mathrm{ss}} - \frac{2\pi}{3}\right) \end{bmatrix} + \begin{bmatrix} \overline{w}^{\Sigma\mathrm{ss}}_{Cz} \\ \overline{w}^{\Sigma\mathrm{ss}}_{Cz} \\ \overline{w}^{\Sigma\mathrm{ss}}_{Cz} \end{bmatrix} + \begin{bmatrix} \delta\overline{w}^{\Sigma\mathrm{ss}}_{Ca} \\ \delta\overline{w}^{\Sigma\mathrm{ss}}_{Cb} \\ \delta\overline{w}^{\Sigma\mathrm{ss}}_{Cc} \end{bmatrix} \\
= & \overline{W}^{\Sigma\mathrm{ss}}_{C} \underline{\sin}(2\omega t + \overline{\phi}^{\Sigma}_{\mathrm{ss}})_{\mathrm{neg}} + \mathbb{1}_3 \overline{w}^{\Sigma\mathrm{ss}}_{Cz} + \delta\overline{w}^{\Sigma\mathrm{ss}}_{Cabc}
\end{aligned} \tag{5}$$

$$\begin{aligned}
w^{\Delta\mathrm{ss}}_{Cabc} \triangleq & \overline{W}^{\Delta\mathrm{ss}}_{C} \begin{bmatrix} \sin\left(\omega t + \overline{\phi}^{\Delta}_{\mathrm{ss}}\right) \\ \sin\left(\omega t + \overline{\phi}^{\Delta}_{\mathrm{ss}} - \frac{2\pi}{3}\right) \\ \sin\left(\omega t + \overline{\phi}^{\Delta}_{\mathrm{ss}} + \frac{2\pi}{3}\right) \end{bmatrix} + \begin{bmatrix} w^{\Delta\mathrm{ss}}_{Cz\alpha} \\ w^{\Delta\mathrm{ss}}_{Cz\alpha} \\ w^{\Delta\mathrm{ss}}_{Cz\alpha} \end{bmatrix} + \begin{bmatrix} \delta\overline{w}^{\Delta\mathrm{ss}}_{Ca} \\ \delta\overline{w}^{\Delta\mathrm{ss}}_{Cb} \\ \delta\overline{w}^{\Delta\mathrm{ss}}_{Cc} \end{bmatrix} \\
= & \overline{W}^{\Delta\mathrm{ss}}_{C} \underline{\sin}(\omega t + \overline{\phi}^{\Delta}_{\mathrm{ss}})_{\mathrm{pos}} + \mathbb{1}_3 w^{\Delta\mathrm{ss}}_{Cz\alpha} + \delta\overline{w}^{\Delta\mathrm{ss}}_{Cabc}
\end{aligned} \tag{6}$$

with the superscript "ss" denoting steady-state variables, the symbol $\overline{\cdot}$ constant variables, and with $\underline{\sin}(\cdot)_{\mathrm{pos}}$ ($\underline{\cos}(\cdot)_{\mathrm{pos}}$) and $\underline{\sin}(\cdot)_{\mathrm{neg}}$ ($\underline{\cos}(\cdot)_{\mathrm{neg}}$) representing vectors of balanced three-phase sine (cosine) signals in positive and negative sequence, respectively. Furthermore, $\overline{W}^{\Sigma\mathrm{ss}}_{C}$ and $\overline{W}^{\Delta\mathrm{ss}}_{C}$ are the energy amplitudes in steady-state, $\overline{\phi}^{\Sigma\mathrm{ss}}$ and $\overline{\phi}^{\Delta\mathrm{ss}}$ their phase-shifts, $\overline{w}^{\Sigma\mathrm{ss}}_{Cz}$ and $w^{\Delta\mathrm{ss}}_{Cz\alpha}$ their common zero-sequence components, whereas $\delta\overline{w}^{\Sigma\mathrm{ss}}_{C}$ and $\delta\overline{w}^{\Delta\mathrm{ss}}_{C}$ are the dc unbalances. More precisely, they are the differences between the dc offset of each phase and the zero-sequence component.

Finally, $w^{\Delta\mathrm{ss}}_{Cz\alpha}$ is the zero-sequence component of $w^{\Delta\mathrm{ss}}_{Cabc}$, which is conveniently defined along with the virtual orthogonal ($\pi/2$ phase shifted) signal $w^{\Delta\mathrm{ss}}_{Cz\beta}$ [6], as:

$$\begin{aligned}
\begin{bmatrix} w^{\Delta\mathrm{ss}}_{Cz\alpha} \\ w^{\Delta\mathrm{ss}}_{Cz\beta} \end{bmatrix} = & \begin{bmatrix} \overline{W}^{\Delta\mathrm{ss}}_{Cz} \sin\left(3\omega t + \overline{\phi}^{\Delta z}_{\mathrm{ss}}\right) \\ \overline{W}^{\Delta\mathrm{ss}}_{Cz} \sin\left(3\omega t + \overline{\phi}^{\Delta z}_{\mathrm{ss}} + \frac{\pi}{2}\right) \end{bmatrix} + \begin{bmatrix} \delta\overline{w}^{\Delta\mathrm{ss}}_{Cz\alpha} \\ \delta\overline{w}^{\Delta\mathrm{ss}}_{Cz\beta} \end{bmatrix} \\
= & \overline{W}^{\Delta\mathrm{ss}}_{Cz} \underline{\sin}(3\omega t + \overline{\phi}^{\Delta z}_{\mathrm{ss}})_{\mathrm{perp}} + \delta\overline{w}^{\Delta\mathrm{ss}}_{Cz\alpha\beta}
\end{aligned} \tag{7}$$

with $\underline{\sin}(\cdot)_{\mathrm{perp}}$ ($\underline{\cos}(\cdot)_{\mathrm{perp}}$) a 2×1 vector containing a sine (cosine) function as well as the same function but with a $\pi/2$ phase shift. Furthermore, $\overline{W}^{\Delta\mathrm{ss}}_{Cz}$ and $\overline{\phi}^{\Delta\mathrm{ss}}_{z}$ are the amplitude and phase-shift of the zero-sequence component of the energy difference in steady-state, and $\delta\overline{w}^{\Delta\mathrm{ss}}_{Cz}$ the term representing its dc offset, which should be regulated to zero.

B. Steady-state variables in dqz coordinates

The equivalent dqz expressions representing the steady-state variables $w^{\Sigma\mathrm{ss}}_{Cabc}$, $w^{\Delta\mathrm{ss}}_{Cabc}$ and $w^{\Delta\mathrm{ss}}_{Cz}$ are obtained by multiplying (5), (6) and (7) respectively by Park transformations at once, twice and three times the grid frequency; i.e., $w^{\Delta\mathrm{ss}}_{Cdqz} = P_{\omega} w^{\Delta\mathrm{ss}}_{Cabc}$, $w^{\Sigma\mathrm{ss}}_{Cdqz} = P_{\text{-}2\omega} w^{\Sigma\mathrm{ss}}_{Cabc}$ and $w^{\Delta\mathrm{ss}}_{CzDQ} = T_{3\omega} w^{\Delta\mathrm{ss}}_{Cz\alpha\beta}$, with P_{ω}, $P_{\text{-}2\omega}$ and $T_{3\omega}$ defined in the Appendix. Thus, the

This is the accepted version of a paper published in 44th Annual Conference of the IEEE Industrial Electronics Society (IECON2018)
DOI: 10.1109/IECON.2018.8592881

$$\mathcal{P}^{\Sigma}_{dqz} \triangleq \begin{bmatrix} -[(v^{\Delta}_{Md}+v^{\Delta}_{MzD})i^{\Delta}_{d} - (v^{\Delta}_{Mq}-v^{\Delta}_{MzQ})i^{\Delta}_{q}]/2 + 2(v^{\Sigma}_{Mz}i^{\Sigma}_{d} + v^{\Sigma}_{Md}i^{\Sigma}_{z}) \\ [(v^{\Delta}_{Md}-v^{\Delta}_{MzD})i^{\Delta}_{q} + (v^{\Delta}_{Mq}+v^{\Delta}_{MzQ})i^{\Delta}_{d}]/2 + 2(v^{\Sigma}_{Mz}i^{\Sigma}_{q} + v^{\Sigma}_{Mq}i^{\Sigma}_{z}) \\ -[(v^{\Delta}_{Md}i^{\Delta}_{d} + v^{\Delta}_{Mq}i^{\Delta}_{q})]/2 + v^{\Sigma}_{Md}i^{\Sigma}_{d} + v^{\Sigma}_{Mq}i^{\Sigma}_{q} + 2v^{\Sigma}_{Mz}i^{\Sigma}_{z} \end{bmatrix} \tag{4a}$$

$$\mathcal{P}^{\Delta}_{dq} \triangleq \begin{bmatrix} -(v^{\Delta}_{Md} + v^{\Delta}_{MzD})i^{\Sigma}_{d} + (v^{\Delta}_{Mq} + v^{\Delta}_{MzQ})i^{\Sigma}_{q} - 2v^{\Delta}_{Md}i^{\Sigma}_{z} + (v^{\Sigma}_{Mz} + v^{\Sigma}_{Md}/2)i^{\Delta}_{d} - (v^{\Sigma}_{Mq}/2)i^{\Delta}_{q} \\ (v^{\Delta}_{Mq} - v^{\Delta}_{MzQ})i^{\Sigma}_{d} + (v^{\Delta}_{Md} - v^{\Delta}_{MzD})i^{\Sigma}_{q} - 2v^{\Delta}_{Mq}i^{\Sigma}_{z} + (v^{\Sigma}_{Mz} - v^{\Sigma}_{Md}/2)i^{\Delta}_{q} - (v^{\Sigma}_{Mq}/2)i^{\Delta}_{d} \end{bmatrix} \tag{4b}$$

$$\mathcal{P}^{\Delta}_{zDQ} \triangleq \begin{bmatrix} -(v^{\Delta}_{Md}i^{\Sigma}_{d} - v^{\Delta}_{Mq}i^{\Sigma}_{q}) + (v^{\Sigma}_{Md}i^{\Delta}_{d} - v^{\Sigma}_{Mq}i^{\Delta}_{q})/2 - 2v^{\Delta}_{MzD}i^{\Sigma}_{z} \\ -(v^{\Delta}_{Md}i^{\Sigma}_{q} + v^{\Delta}_{Mq}i^{\Sigma}_{d}) + (v^{\Sigma}_{Mq}i^{\Delta}_{d} + v^{\Sigma}_{Md}i^{\Delta}_{q})/2 - 2v^{\Delta}_{MzQ}i^{\Sigma}_{z} \end{bmatrix} \tag{4c}$$

expressions of the energy variables in (5), (6) and (7) become:

$$\begin{aligned} w^{\Sigma\mathsf{ss}}_{Cdqz} =& P_{\text{-}2\omega}\left[\overline{W}^{\Sigma\mathsf{ss}}_{C}\underline{\sin}(2\omega t + \overline{\phi}^{\Sigma}_{\mathsf{ss}})_{\text{neg}} + \mathbb{1}_3\overline{w}^{\Sigma\mathsf{ss}}_{Cz} + \delta\overline{w}^{\Sigma\mathsf{ss}}_{Cabc}\right] \\ =& \begin{bmatrix} \overline{w}^{\Sigma\mathsf{ss}}_{Cd} \\ \overline{w}^{\Sigma\mathsf{ss}}_{Cq} \\ 0 \end{bmatrix} + \begin{bmatrix} 0 \\ 0 \\ \overline{w}^{\Sigma\mathsf{ss}}_{Cz} \end{bmatrix} + P_{\text{-}2\omega}\begin{bmatrix} \delta\overline{w}^{\Sigma\mathsf{ss}}_{Ca} \\ \delta\overline{w}^{\Sigma\mathsf{ss}}_{Cb} \\ \delta\overline{w}^{\Sigma\mathsf{ss}}_{Cc} \end{bmatrix} \\ =& \overline{w}^{\Sigma\mathsf{ss}}_{Cdqz} + \frac{2}{3}\begin{bmatrix} \mathbb{1}_3^{\top}\text{diag}(\delta\overline{w}^{\Sigma\mathsf{ss}}_{Cabc})\underline{\cos}(2\omega t)_{\text{neg}} \\ -\mathbb{1}_3^{\top}\text{diag}(\delta\overline{w}^{\Sigma\mathsf{ss}}_{Cabc})\underline{\sin}(2\omega t)_{\text{neg}} \\ 0 \end{bmatrix} \end{aligned} \tag{8}$$

$$\begin{aligned} w^{\Delta\mathsf{ss}}_{Cdqz} =& P_{\omega}\left[\overline{W}^{\Delta\mathsf{ss}}_{C}\underline{\sin}(\omega t + \overline{\phi}^{\Delta}_{\mathsf{ss}})_{\text{pos}} + \mathbb{1}_3 w^{\Delta\mathsf{ss}}_{Cz\alpha} + \delta\overline{w}^{\Delta\mathsf{ss}}_{Cabc}\right] \\ =& \begin{bmatrix} \overline{w}^{\Delta\mathsf{ss}}_{Cd} \\ \overline{w}^{\Delta\mathsf{ss}}_{Cq} \\ 0 \end{bmatrix} + \begin{bmatrix} 0 \\ 0 \\ w^{\Delta\mathsf{ss}}_{Cz\alpha} \end{bmatrix} + P_{\omega}\begin{bmatrix} \delta\overline{w}^{\Delta\mathsf{ss}}_{Ca} \\ \delta\overline{w}^{\Delta\mathsf{ss}}_{Cb} \\ \delta\overline{w}^{\Delta\mathsf{ss}}_{Cc} \end{bmatrix} \\ =& \overline{w}^{\Delta\mathsf{ss}}_{Cdqz} + \frac{2}{3}\begin{bmatrix} \mathbb{1}_3^{\top}\text{diag}(\delta\overline{w}^{\Delta\mathsf{ss}}_{Cabc})\underline{\cos}(\omega t)_{\text{pos}} \\ \mathbb{1}_3^{\top}\text{diag}(\delta\overline{w}^{\Delta\mathsf{ss}}_{Cabc})\underline{\sin}(\omega t)_{\text{pos}} \\ 0 \end{bmatrix} \end{aligned} \tag{9}$$

$$\begin{aligned} w^{\Delta\mathsf{ss}}_{CzDQ} =& T_{3\omega}\left[\overline{W}^{\Delta\mathsf{ss}}_{Cz}\underline{\sin}(3\omega t + \overline{\phi}^{\Delta z}_{\mathsf{ss}})_{\text{perp}} + \delta\overline{w}^{\Delta\mathsf{ss}}_{Cz\alpha\beta}\right] \\ =& \overline{w}^{\Delta\mathsf{ss}}_{CzDQ} + T_{3\omega}\delta\overline{w}^{\Delta\mathsf{ss}}_{Cz\alpha\beta} \\ =& \overline{w}^{\Delta\mathsf{ss}}_{CzDQ} + \begin{bmatrix} \mathbb{1}_2^{\top}\text{diag}(\delta\overline{w}^{\Delta\mathsf{ss}}_{Cz\alpha\beta})\underline{\cos}(3\omega t)_{\text{perp}} \\ \mathbb{1}_2^{\top}\text{diag}(\delta\overline{w}^{\Delta\mathsf{ss}}_{Cz\alpha\beta})\underline{\sin}(3\omega t)_{\text{perp}} \end{bmatrix} \end{aligned} \tag{10}$$

with $\text{diag}(x) \triangleq \begin{bmatrix} x_1 & 0 & 0 \\ 0 & \ddots & 0 \\ 0 & 0 & x_n \end{bmatrix}$ for a generic vector x.

The above equations reveal that the dc unbalances between the energy variables in abc coordinates appear in dq coordinates multiplying a Park transformation as in the last term of (8), (9) and (10). Therefore, the resulting products are, in fact, oscillatory terms with the same frequency of their respective Park transforms, whereas the rest of the terms are constant. Thus, removing dc unbalances in the stationary frame turns into suppressing the steady-state oscillations in the corresponding Synchronously Rotating Reference Frame (SRRF). Then, the energy balancing control objective translates into forcing the energy variables in dqz coordinates to remain constants; i.e., $w^{\Sigma\mathsf{ss}}_{Cdqz} \equiv \overline{w}^{\Sigma\mathsf{ss}}_{Cdqz}$, $w^{\Delta\mathsf{ss}}_{Cdq} \equiv \overline{w}^{\Delta\mathsf{ss}}_{Cdq}$ and $w^{\Delta\mathsf{ss}}_{CzDQ} \equiv \overline{w}^{\Delta\mathsf{ss}}_{CzDQ}$, by eliminating the steady state oscillation terms.

IV. Energy Balancing Control Design

In addition to performing standard active and reactive power control, as well as regulation of the total energy stored in the converter ($3\cdot w^{\Sigma}_{Cz}$) to a desired reference, the proposed control strategy eliminates the oscillations in w^{Δ}_{Cdq}, w^{Δ}_{CzDQ} and w^{Σ}_{Cdq} via outer-loops, as depicted in Fig. 2. Indeed, the task of each energy outer loop needs to be associated to an inner loop for correct operation. Nonetheless, as suggested by Fig. 2, it may seem still rather unclear which current to use to control each energy variable. To overcome this limitation, the following approximations on the MMC model from (3) are introduced, which will allow for a better insight on the converter dynamics, thus, simplifying the control design.

A. Approximations for the control design

The following approximations are performed, aiming at simplifying the terms defined by (4a), (4b) and (4c).

- A2. Since $v^{\Sigma}_{Mdq} << v^{\Sigma}_{Mz}$, assume that $v^{\Sigma}_{Mdq} \approx 0$ and that $v^{\Sigma}_{Mz} \approx \overline{v}_{dc}/2$. These assumptions eliminate several of the nonlinear products present in (4).
- A3. Assume that v^{Δ}_{Md} acts as a constant and that $v^{\Delta}_{Mq} \approx 0$, in the capacitive energy dynamics.
- A4. When the outer loop control of an energy variable is being designed using i^{Σ}_{dqz} as the control output, assume that the grid currents i^{Δ}_{dq} acts as a measurable disturbance.
- A5. Similarly, when the outer loop control of a particular energy variable is being designed using i^{Δ}_{dq} as the control output, assume that the circulating currents i^{Σ}_{dqz} act as a measurable disturbance.
- A6. Given that usually $v^{\Delta}_{Mdq} >> v^{\Delta}_{MzDQ}$, whenever these two components are adding each other, assume that $v^{\Delta}_{MzDQ} \approx 0$.

Under the above approximations, the capacitor dynamics of the MMC can be simplified by replacing the definitions given in (4) by:

$$\mathcal{P}^{\Sigma}_{dqz} \approx \begin{bmatrix} -v^{\Delta}_{Md}i^{\Delta}_{d}/2 + v_{dc}i^{\Sigma}_{d} \\ v^{\Delta}_{Md}i^{\Delta}_{q}/2 + v_{dc}i^{\Sigma}_{q} \\ -v^{\Delta}_{Md}i^{\Delta}_{d}/2 + v_{dc}i^{\Sigma}_{z} \end{bmatrix} \tag{11a}$$

$$\mathcal{P}^{\Delta}_{dq} \approx \begin{bmatrix} -v^{\Delta}_{Md}i^{\Sigma}_{d} - 2v^{\Delta}_{Md}i^{\Sigma}_{z} + v_{dc}i^{\Delta}_{d}/2 \\ v^{\Delta}_{Md}i^{\Sigma}_{q} + v_{dc}i^{\Delta}_{q}/2 \end{bmatrix} \tag{11b}$$

This is the accepted version of a paper published in 44th Annual Conference of the IEEE Industrial Electronics Society (IECON2018)
DOI: 10.1109/IECON.2018.8592881

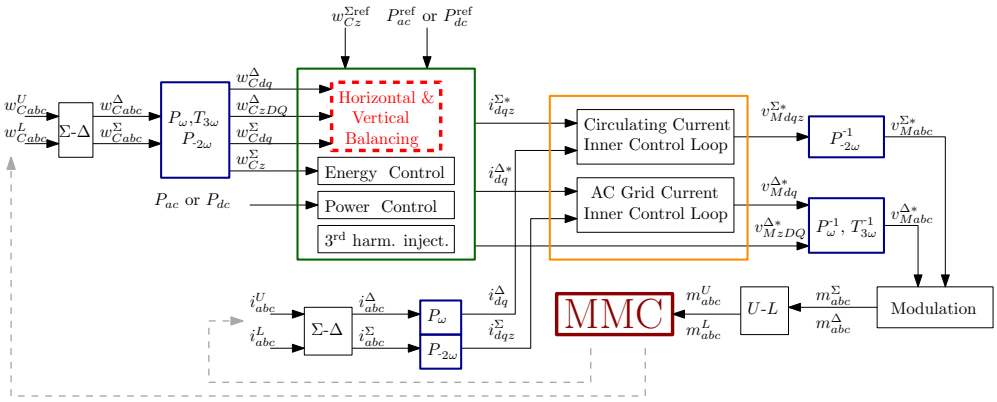

Fig. 2. Control System Overview

$$\mathcal{P}^{\Delta}_{zDQ} \approx \begin{bmatrix} -v^{\Delta}_{Md} i^{\Sigma}_{d} - 2v^{\Delta}_{MzD} i^{\Sigma}_{z} \\ -v^{\Delta}_{Md} i^{\Sigma}_{q} - 2v^{\Delta}_{MzQ} i^{\Sigma}_{z} \end{bmatrix} \tag{11c}$$

B. Analysis of Outer-Loop Control Options

The steady-state analysis of section III demonstrated the need for eliminating the oscillatory terms at the appropriate frequency from the respective energy variables. In order to achieve this objective, the active damping method applied in [25], [26] is used in this paper. However, given the multiple degrees of freedom in the control of MMCs, several alternatives for achieving the same objective exists.

As a first example, the case of the energy sum w^{Σ}_{Cdq} is considered. Inspecting the dynamics of w^{Σ}_{Cdq} from the first equation in (3a), but using the approximated version of $\mathcal{P}^{\Sigma}_{dq}$ given in (11a), reveals that the outer loop design for this variable could be performed by using as the control variable either i^{Δ}_{dq} or i^{Σ}_{dq}, since both are directly proportional to $\dot{w}^{\Sigma}_{Cdq}$.

A similar observation can be drawn with respect to the case of w^{Δ}_{Cdq} where the dynamics are analyzed by means of the third equation in (3a) but using the approximated version of $\mathcal{P}^{\Delta}_{dq}$ given in (11b). Here it is again possible to choose as a control variable either i^{Δ}_{dq} or i^{Σ}_{dq} since both are directly proportional to $\dot{w}^{\Delta}_{Cdq}$.

Finally, a different conclusion arises when analyzing the dynamics of w^{Δ}_{CzDQ} from the fourth equation given in (3a), under the approximated version of $\mathcal{P}^{\Delta}_{zDQ}$ given in (11c). First, it should be noted that i^{Δ}_{dq} cannot be used as a control output variable of the outer loop for w^{Δ}_{CzDQ} while, i^{Σ}_{dq} appears directly proportional to $\dot{w}^{\Delta}_{CzDQ}$ and can be used instead. In addition, the control voltages v^{Δ}_{MzDQ} could also be used for the same purpose, although it would imply a third harmonic injection [27].

Remark 4: Notice that i^{Σ}_{z} also appears as a proportional term in the dynamics of w^{Δ}_{Cdq} and w^{Δ}_{CzDQ}. Therefore, it could be argued to consider this current as a potential control output for the outer loop designs. However, it does not seem suitable for independent control of the energy dq components, and will therefore not be considered further as a control output option.

C. Proposed Outer Loop Control by Active Damping

Based on the analysis from the previous subsection, two alternatives are possible for each outer loop corresponding to an energy variable dq component, yielding 2^6 combinations. For the sake of compactness, this paper will limit the analysis to the following two options.

1) Case A–Energy balancing via i^{Σ}_{dq}: In this case, the outer loop controller outputs are added to each other such that only the circulating current i^{Σ}_{dq} is used to achieve all of the damping objectives, as it is the only variable that appears directly proportional to all the the energy dynamics of interest under the considered approximations. By invoking a linear superposition assumption (A8.), the outer loop takes the form indicated in (12), with $D^{\Sigma}_{2\omega} \triangleq \bar{D}^{\Sigma}_{2\omega}\mathbb{I}_2$, $D^{\Delta}_{\omega} \triangleq \bar{D}^{\Delta}_{\omega}\mathrm{diag}(1,-1)$ and $D^{\Delta}_{3\omega} \triangleq \bar{D}^{\Delta}_{3\omega}\mathbb{I}_2$ representing the constant damping coefficient matrices, $\mathbb{I}_2 \in \mathbb{R}^2$ the identity matrix, and the symbol $\hat{}$ indicating the unwanted oscillations of each energy component. These oscillations can be isolated via filtering, as shown in the Appendix. The resulting control structure is illustrated in Fig. 3

$$i^{\Sigma *}_{dq} = i^{\Sigma,\mathrm{ref}}_{dq} - D^{\Sigma}_{2\omega}\frac{\hat{w}^{\Sigma}_{Cdq}}{v_{dc}} + D^{\Delta}_{\omega}\frac{\hat{w}^{\Delta}_{Cdq}}{(v_{dc}/2)} + D^{\Delta}_{3\omega}\frac{\hat{w}^{\Delta}_{CzDQ}}{2i^{\Sigma}_{z}} \tag{12}$$

This control scheme, albeit completely coupled, releases the active current i^{Δ}_{d} from energy balancing purposes and does not require any third harmonic injection.

2) Case B–Energy Balancing via i^{Σ}_{dq}, i^{Δ}_{dq} and v^{Δ}_{MzDQ}: Another alternative is to select the outer loop control outputs such that each one will be associated to only one energy variable as shown in (13) and illustrated in Fig. 4, but now taking $D^{\Delta}_{\omega} \triangleq \bar{D}^{\Delta}_{\omega}\mathbb{I}_2$ instead. This strategy uses the circulating current i^{Σ}_{dq} to damp the 2ω oscillations of w^{Σ}_{Cdq}, the grid current i^{Δ}_{dq} to damp the oscillations at ω of w^{Δ}_{Cdq} and the zero sequence third harmonic injection voltage v^{Δ}_{MzDQ} to damp the 3ω oscillations of w^{Δ}_{CzDQ}.

$$i^{\Sigma *}_{dq} = \underbrace{i^{\Sigma,\mathrm{ref}}_{dq}}_{\text{reference}} \underbrace{- D^{\Sigma}_{2\omega}\frac{\hat{w}^{\Sigma}_{Cdq}}{v_{dc}}}_{\text{damping}} \tag{13a}$$

This is the accepted version of a paper published in 44th Annual Conference of the IEEE Industrial Electronics Society (IECON2018)
DOI: 10.1109/IECON.2018.8592881

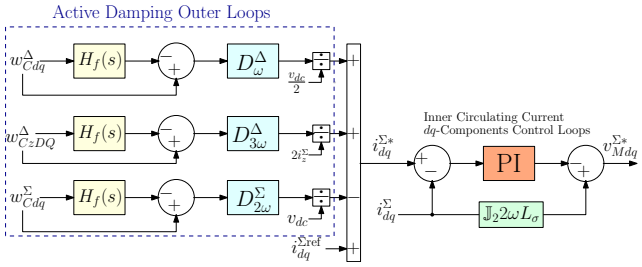

Fig. 3. Case A–Energy balancing via i^{Σ}_{dq}

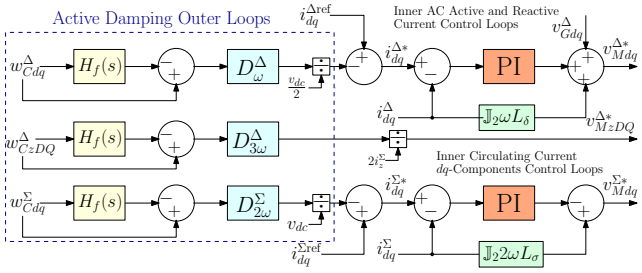

Fig. 4. Case B–Energy Balancing via i^{Σ}_{dq}, i^{Δ}_{dq} and v^{Δ}_{MzDQ}

$$i^{\Delta *}_{dq} = \underbrace{i^{\Delta,\mathrm{ref}}_{dq}}_{\text{reference}} - \underbrace{D^{\Delta}_{\omega}\frac{\hat{w}^{\Delta}_{Cdq}}{(v_{dc}/2)}}_{\text{damping}} \tag{13b}$$

$$v^{\Delta *}_{MzDQ} = \underbrace{v^{\Delta,\mathrm{ref}}_{MzDQ}}_{\text{reference}} + \underbrace{D^{\Delta}_{3\omega}\frac{\hat{w}^{\Delta}_{CzDQ}}{2i^{\Sigma}_{z}}}_{\text{damping}} \tag{13c}$$

The potential of this strategy lies in its decoupled structure. However, notice that this strategy requires the active current i^{Δ}_{d}, associated to the active power transfer of the system, to be controlled to achieve the desired damping. Furthermore, it also requires a third harmonic voltage injection.

D. Brief discussion on the w^{Σ}_{Cz} outer-loop

In addition to the energy balancing outer-loops discussed in the previous subsection, it is worth analyzing the zero-sequence energy sum w^{Σ}_{Cz} dynamics expressed by the second equation in (3a), but considering the approximated definition of $\mathcal{P}^{\Sigma}_{z}$ given in (4a). This equation reveals that w^{Σ}_{Cz} can be controlled either by acting on i^{Σ}_{z} or i^{Δ}_{d}, which is a result that has been already reported in the literature [28].

V. Simulation Results

To evaluate the control performance, a time domain simulation with an MMC in a single-terminal HVDC configuration is carried out. The same circuit parameters as in [19] are adopted. The scenario begins with the MMC transferring 0.8 pu (out of 1 GW) of active power P_{ac}. At this steady-state condition, only the zero-sequence energy sum controller is active (i.e. for w^{Σ}_{z}). Then, at $t = 0.5$ s, a step of 0.2 pu is applied to the reactive power reference, which naturally creates an energy unbalance inside the MMC. At $t = 1$ s, one of the two balancing methods

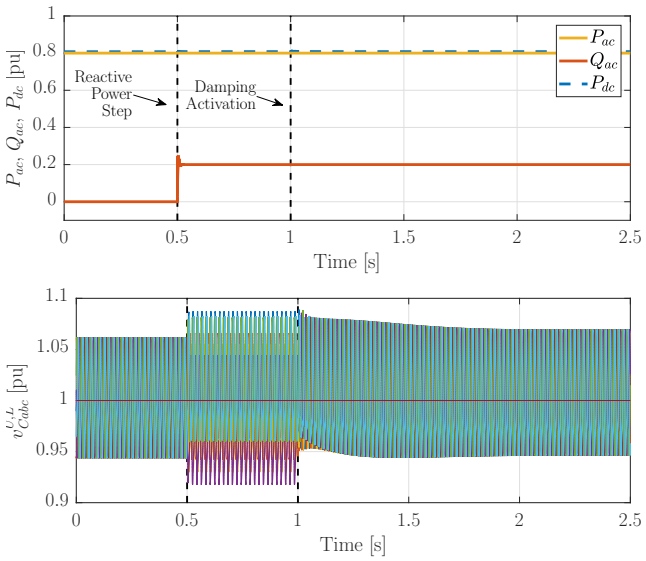

Fig. 5. Case A - MMC power response and arm capacitor voltages

proposed in the previous section (i.e., case A or B) is activated to evaluate the response of the system.

1) Case A–Energy balancing via i^{Σ}_{dq}: Results of the active and reactive powers and the arm capacitor voltages in abc coordinates are depicted in Fig. 5 for the energy balancing strategy from Fig. 3. As expected, the ac and dc power responses are decoupled from the reactive power. Moreover, at the bottom of Fig. 5, unbalances are observed on the upper and lower equivalent arm capacitor voltages $v^{U,L}_{Cabc}$ immediately after the reactive power step occurs. Nonetheless, when the energy balancing method is activated, the voltages return to a balanced condition.

In order to gain a better understanding on the adopted control strategy performance in dqz coordinates, Figs. 6 and 7 show the simulation results of the energy sum and difference in their respective SRRFs under the same scenario. When the system is perturbed by the reactive power step, the undesired energy unbalances appear as oscillations in the SRRF as observed in the figures between $t = 0.5$ s and 1 s. Furthermore, when the energy balancing control under consideration is enabled, the oscillations on the energy variables disappear implying the return of the system to a balanced condition.

2) Case B–Energy Balancing via i^{Σ}_{dq}, i^{Δ}_{dq} and v^{Δ}_{MzDQ}: The same simulation scenario is repeated but with the energy balancing control from Fig. 4. As for Case A, results of the active and reactive powers and upper and lower equivalent arm capacitance voltages $v^{U,L}_{Cabc}$ are shown in Fig. 8. For $t < 1$ s, the same response as in Fig. 5 is observed. However, when the energy balancing control is enabled, the ac and dc powers are perturbed as well as the reactive power. This is due to the fact that the control for w^{Δ}_{Cdq} is carried on with the manipulation of the grid currents i^{Δ}_{dq}. The dynamic responses of w^{Σ}_{Cdqz}, w^{Δ}_{Cdq} and w^{Δ}_{CzDQ} are similar to those from Case A, and are omitted for brevity.

This is the accepted version of a paper published in 44th Annual Conference of the IEEE Industrial Electronics Society (IECON2018)
DOI: 10.1109/IECON.2018.8592881

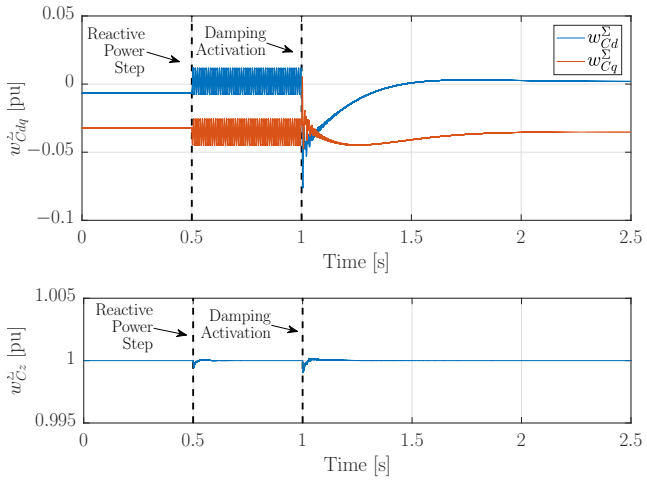

Fig. 6. Case A - Equivalent arm capacitance energy sum w^{Σ}_{Cdqz}

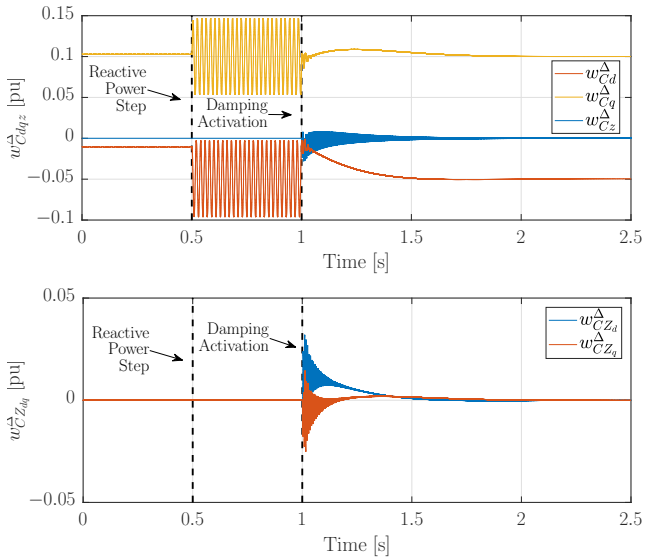

Fig. 7. Case A - Equivalent arm capacitance energy difference w^{Δ}_{Cdqz} and w^{Δ}_{CzDQ}

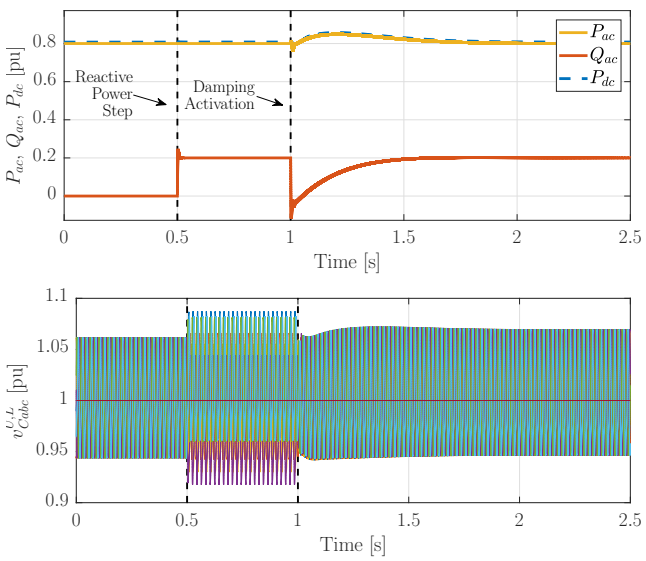

Fig. 8. Case B- MMC power response and arm capacitor voltages

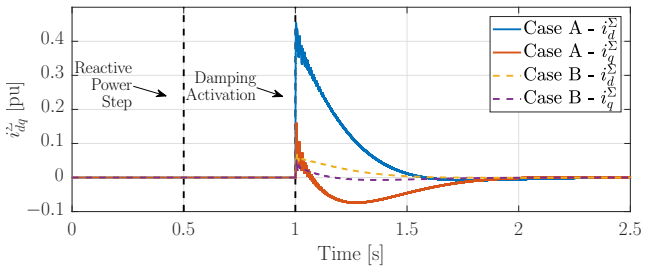

Fig. 9. Comparison of circulating current response from Case A and Case B

When operating under the energy balancing control strategy of Case B, the decoupling between the ac and dc powers is lost. This coupling could be avoided by controlling the dc power to a constant by means of i^{Σ}_{z} and using i^{Δ}_{d} to regulate w^{Σ}_{z}, as suggested in [28]. However, even under such a scenario, the ac active power would be dynamically perturbed, and there would be a stronger influence on w^{Σ}_{z} than when operating under the strategy of Case A, which is arguably not always convenient. Conversely, as revealed by a comparison between the circulating current responses in Fig. 9, the energy balancing strategy of Case B demands significantly lower circulating currents during transients.

VI. Conclusions

This paper presents an MMC control approach for vertical and horizontal energy balancing control in dqz coordinates. The design procedure is based on a recently presented state-space representation of the converter in multiple synchronously rotating reference frames (SRRF) [6]. Since the model uses energy variables for the arm capacitor dynamics and assumes linear current dynamics, it becomes particularly useful for designing energy controllers based on linear inner current control loops. Moreover, this model is further manipulated with a series of justified assumptions that yield in a simplified model which provides a significant amount of insight on the internal energy dynamics of an MMC. This insight is further exploited for designing a family of outer-loop controller strategies. More precisely, by proving that vertical and horizontal energy imbalances are represented by undesired oscillations in the multiple SRRF, a simple method for active damping control is used to dissipate them and achieve the desired energy balancing.

As an example of the gained insight, two possibilities of outer loop controllers based on active damping are compared. The first option consists of assigning the full responsibility of the vertical and horizontal balancing to the dq-components of the circulating current, while the second option shares this task among the dq-components of the circulating currents, the ac-grid currents and a third harmonic zero sequence voltage injection. By simulation it was demonstrated how the strategy

This is the accepted version of a paper published in 44th Annual Conference of the IEEE Industrial Electronics Society (IECON2018)
DOI: 10.1109/IECON.2018.8592881

that distributes the damping control between multiple current and voltage components had better performance at the price of relying dynamically on the ac-side active and reactive currents. On the other hand, the option relying only on the dq-components of the circulating currents achieves the energy balancing objectives without the need of perturbing the ac-side current references and the third harmonic injection.

APPENDIX

A. Park transforms used in the derivation

The Park transformations used in this paper are based on the expression of $P_{n\omega}$ given below, for $n = 1$ and $n = -2$.

$$P_{n\omega} \triangleq \frac{2}{3}\begin{bmatrix} \cos(n\omega t) & \cos(n\omega t - 2\pi/3) & \cos(n\omega t + 2\pi/3) \\ \sin(n\omega t) & \sin(n\omega t - 2\pi/3) & \sin(n\omega t + 2\pi/3) \\ 1/2 & 1/2 & 1/2 \end{bmatrix}$$

In addition, the following rotational transform was used.

$$T_{3\omega} \triangleq \begin{bmatrix} \cos(3\omega t) & \sin(3\omega t) \\ \sin(3\omega t) & -\cos(3\omega t) \end{bmatrix}$$

B. Energy Filtering

The oscillatory part of the dq (and DQ) energy variables can be isolated by first order low pass filters as indicated by a generic variable x in the frequency domain as:

$$\hat{x} \triangleq x - H_f(s)x, \quad H_f(s) \triangleq \frac{\omega_f}{s + \omega_f}, \tag{14}$$

with the symbol $\hat{\cdot}$ denoting the oscillatory part of x. Please note that any suitable filter function could be used as $H_f(s)$.

REFERENCES

[1] A. Lesnicar and R. Marquardt, "An innovative modular multilevel converter topology suitable for a wide power range," in *Proc. IEEE PowerTech Bologna*, vol. 3, June 2003, p. 6 pp. Vol.3.

[2] A. Antonopoulos, L. Angquist, and H. P. Nee, "On dynamics and voltage control of the modular multilevel converter," in *Proc. of the 13th European Conf. on Power Electron. and Appl.*, Sept 2009, pp. 1–10.

[3] A. E. Leon and S. J. Amodeo, "Energy balancing improvement of modular multilevel converters under unbalanced grid conditions," *IEEE Trans. on Power Electron.*, vol. 32, no. 8, pp. 6628–6637, Aug 2017.

[4] L. Harnefors, A. Antonopoulos, S. Norrga, L. Angquist, and H. P. Nee, "Dynamic analysis of modular multilevel converters," *IEEE Trans. on Industrial Electronics*, vol. 60, no. 7, pp. 2526–2537, July 2013.

[5] G. Bergna, J. A. Suul, and S. D'Arco, "Small-signal state-space modeling of modular multilevel converters for system stability analysis," in *2015 IEEE Energy Conversion Congress and Exposition (ECCE)*, Sept 2015, pp. 5822–5829.

[6] G. Bergna-Diaz, J. A. Suul, and S. D'Arco, "Energy-based state-space representation of modular multilevel converters with a constant equilibrium point in steady-state operation," *IEEE Transactions on Power Electronics*, vol. 33, no. 6, pp. 4832–4851, June 2018.

[7] S. Yang, P. Wang, and Y. Tang, "Feedback linearization-based current control strategy for modular multilevel converters," *IEEE Transactions on Power Electronics*, vol. 33, no. 1, pp. 161–174, Jan 2018.

[8] G. Bergna, J. A. Suul, and S. D'Arco, "State-space modelling of modular multilevel converters for constant variables in steady-state," in *2016 IEEE 17th Workshop on Control and Modeling for Power Electronics (COMPEL)*, June 2016, pp. 1–9.

[9] Q. Tu, Z. Xu, and L. Xu, "Reduced switching-frequency modulation and circulating current suppression for modular multilevel converters," in *Transmission and Distribution Conference and Exposition (T D), 2012 IEEE PES*, May 2012, pp. 1–1.

[10] ——, "Reduced switching-frequency modulation and circulating current suppression for modular multilevel converters," *IEEE Trans. on Power Delivery*, vol. 26, no. 3, pp. 2009–2017, July 2011.

[11] J. Freytes, G. Bergna, J. A. Suul, S. D'Arco, F. Gruson, F. Colas, H. Saad, and X. Guillaud, "Improving small-signal stability of an MMC with CCSC by control of the internally stored energy," *IEEE Transactions on Power Delivery*, vol. 33, no. 1, pp. 429–439, Feb 2018.

[12] G. Bergna, E. Berne, P. Egrot, P. Lefranc, A. Arzande, J.-C. Vannier, and M. Molinas, "An energy-based controller for HVDC modular multilevel converter in decoupled double synchronous reference frame for voltage oscillation reduction," *Industrial Electronics, IEEE Trans. on*, vol. 60, no. 6, pp. 2360–2371, June 2013.

[13] G. Bergna, J. A. Suul, E. Berne, P. Egrot, J. C. Vannier, and M. Molinas, "Generalized abc frame differential current control ensuring constant dc power for modular multilevel converters under unbalanced operation," in *2013 15th European Conference on Power Electronics and Applications (EPE)*, Sept 2013, pp. 1–10.

[14] G. Bergna, A. Garcés, E. Berne, P. Egrot, A. Arzandé, J. C. Vannier, and M. Molinas, "A generalized power control approach in abc frame for modular multilevel converter HVDC links based on mathematical optimization," *IEEE Transactions on Power Delivery*, vol. 29, no. 1, pp. 386–394, Feb 2014.

[15] H. R. Parikh, R. S. M. Loeches, G. Tsolaridis, R. Teodorescu, L. Mathe, and S. Chaudhary, "Capacitor voltage ripple reduction and arm energy balancing in MMC-HVDC," in *Proc. 2016 IEEE 16th Int. Conf. on Environment and Electrical Eng. (EEEIC)*, June 2016, pp. 1–6.

[16] M. Jankovic, A. Costabeber, A. Watson, and J. C. Clare, "Arm-balancing control and experimental validation of a grid-connected mmc with pulsed dc load," *IEEE Transactions on Industrial Electronics*, vol. 64, no. 12, pp. 9180–9190, Dec 2017.

[17] J. Freytes, G. Bergna, J. A. Suul, S. D'Arco, H. Saad, and X. Guillaud, "State-space modelling with steady-state time invariant representation of energy based controllers for modular multilevel converters," in *2017 IEEE Manchester PowerTech*, June 2017, pp. 1–7.

[18] H. Fehr and A. Gensior, "Improved energy balancing for grid side modular multilevel converters by optimized feed-forward circulating currents and common-mode voltage," *IEEE Transactions on Power Electronics*, pp. 1–1, 2018.

[19] G. Bergna-Diaz, J. Freytes, X. Guillaud, S. D'Arco, and J. A. Suul, "Generalized voltage-based state-space modeling of modular multilevel converters with constant equilibrium in steady state," *IEEE Journal of Emerging and Selected Topics in Power Electronics*, vol. 6, no. 2, pp. 707–725, June 2018.

[20] P. Kundur, *Power System Stability and Control*. New York, USA: McGraw-Hill, 1994.

[21] P. Dorato, V. Cerone, and C. Abdallah, *Linear-Quadratic Control: An Introduction*. New York, NY, USA: Simon & Schuster, Inc., 1994.

[22] H. K. Khalil, *Nonlinear systems*. Upper Saddle River, (N.J.): Prentice Hall, 1996.

[23] S. Rohner, J. Weber, and S. Bernet, "Continuous model of modular multilevel converter with experimental verification," in *2011 IEEE Energy Conversion Congress and Exposition*, Sept 2011, pp. 4021–4028.

[24] H. Saad, X. Guillaud, J. Mahseredjian, S. Dennetière, and S. Nguefeu, "MMC capacitor voltage decoupling and balancing controls," *IEEE Trans. on Power Delivery*, vol. 30, no. 2, pp. 704–712, April 2015.

[25] M. Malinowski and M. P. Kazmierkowski, "Damping of resonance in three-phase PWM converter with lcl filter," in *Proceedings of the 2005 IEEE International Conference on Industrial Technology, ICIT 2005*, Dec. 2005, pp. 861–865.

[26] S. D'Arco, J. A. Suul, and M. Molinas, "Implementation and analysis of a control scheme for damping of oscillations in VSC-based HVDC grids," in *Proc. of the 16th International Power Electronics and Motion Control Conference and Exposition, PEMC 2014*, Sept 2014, pp. 586–593.

[27] J. A. Houldsworth and D. A. Grant, "The use of harmonic distortion to increase the output voltage of a three-phase PWM inverter," *IEEE Trans. on Industry Applications*, vol. IA-20, no. 5, pp. 1224–1228, Sept 1984.

[28] G. Bergna, J. A. Suul, and S. D'Arco, "Impact on small-signal dynamics of using circulating currents instead of ac-currents to control the dc voltage in mmc hvdc terminals," in *2016 IEEE Energy Conversion Congress and Exposition (ECCE)*, Sept 2016, pp. 1–8.

This is the accepted version of a paper published in 44th Annual Conference of the IEEE Industrial Electronics Society (IECON2018)
DOI: 10.1109/IECON.2018.8592881